Circulating microRNA signature for the diagnosis of very high-risk prostate cancer

Ali H. Alhasan[a,b,1], Alexander W. Scott[b,c,1], Jia J. Wu[a], Gang Feng[d], Joshua J. Meeks[e,f,2], C. Shad Thaxton[b,e,f,g,2], and Chad A. Mirkin[a,b,c,h,2]

[a]Interdepartmental Biological Sciences Program, Northwestern University, Evanston, IL 60208; [b]International Institute for Nanotechnology, Northwestern University, Evanston, IL 60208; [c]Department of Biomedical Engineering, Northwestern University, Evanston, IL 60208; [d]Health and Biomedical Informatics Division, Department of Preventive Medicine, Feinberg School of Medicine, Northwestern University, Chicago, IL 60611; [e]Department of Urology, Feinberg School of Medicine, Northwestern University, Chicago, IL 60611; [f]Robert H. Lurie Comprehensive Cancer Center, Northwestern University, Chicago, IL 60611; [g]Institute for BioNanotechnology and Medicine, Northwestern University, Chicago, IL 60611; and [h]Department of Chemistry, Northwestern University, Evanston, IL 60208

Contributed by Chad A. Mirkin, July 18, 2016 (sent for review May 7, 2016; reviewed by Shuming Nie and Norm Smith)

We report the identification of a molecular signature using the Scano-miR profiling platform based on the differential expression of circulating microRNAs (miRNA, miR) in serum samples specific to patients with very high-risk (VHR) prostate cancer (PCa). Five miRNA PCa biomarkers (miR-200c, miR-605, miR-135a*, miR-433, and miR-106a) were identified as useful for differentiating indolent and aggressive forms of PCa. All patients with VHR PCa in the study had elevated serum levels of miR-200c. Circulating miR-433, which was differentially expressed in patients with VHR versus low-risk (LR) forms of PCa, was not detectable by quantitative real-time PCR in samples from healthy volunteers. In blind studies, the five miRNA PCa biomarkers were able to differentiate patients with VHR PCas from those with LR forms as well as healthy individuals with at least 89% accuracy. Biological pathway analysis showed the predictive capability of these miRNA biomarkers for the diagnosis and prognosis of VHR aggressive PCa.

prostate cancer | microRNA | Scano-miR | spherical nucleic acid | biomarker

Prostate cancer (PCa) is the most common noncutaneous malignancy among men in the United States and the second most common cause of cancer mortality (1, 2). Despite the prevalence of PCa, there are no specific and accurate diagnostic or prognostic biomarkers to differentiate tumor aggressiveness. Although serum prostate-specific antigen (PSA) concentration is used as a routine screening tool for PCa, up to 11% of men with a PSA < 2.0 ng/mL may still have PCa, and based on the serum level alone, it is not possible to distinguish between high- and low-risk (LR) PCas (3). Due to the lack of specificity with PSA-based screening and harm associated with overtreatment and overdiagnosis, the US Preventive Services Task Force recommended physicians do not routinely perform PSA-based PCa screening (4–6). The major criticism associated with PSA-based screening is "overtreatment." This may be reduced by improved risk stratification; men with LR and very low-risk (VLR) PCa can be monitored on active surveillance, whereas those with intermediate and high-risk (HR) PCa benefit from treatment (7–11). Treatment can be avoided in almost 70% of men in active surveillance at 15 y of follow-up (12). However, many urologists and patients are reluctant to monitor their cancer on active surveillance due to concerns for delaying treatment or potentially missing treatment of aggressive cancer during a window of cure. Evidence for inadequacy of staging and risk stratification is demonstrated by the increase in Gleason Grade from Gleason 6–7 or higher in 40% of patients treated with radical prostatectomy (RP) (13, 14). Thus, significant discrepancies between prostate needle biopsy and RP specimens may be attributed to diagnostic pitfalls as only 2% of the prostate is sampled with a biopsy (15). Improved staging, which can result in reduction in overtreatment, patient anxiety, and biopsy-related complications, can be achieved by identifying unique molecular signatures capable of discriminating aggressive forms of PCa (16).

Detection of molecular signatures that are indicative of molecular processes related to aggressive forms of PCa may allow biological insight into differentiating aggressive from indolent PCa. MicroRNAs (miRNA, miR) are critical gene regulatory elements that are present in stable forms in serum and have emerged as potential noninvasive biomarkers for cancer diagnosis (17–21). Exosomes may function as delivery vehicles of circulating miRNAs and transport them from primary cancer sites to metastatic sites while also shielding miRNAs from serum nucleases (22, 23). Therefore, serum exosomal miRNAs may potentially serve as noninvasive biomarkers to identify molecular signatures specific to patients with a higher risk of developing aggressive forms of PCa relative to those with indolent PCa. It is important to note that others have identified miRNA signatures and linked them to PCa progression. Circulating miR-141, miR-200c, and miR-375 have been proposed as potential blood markers for the diagnosis of PCa (20, 24, 25). However, the heterogeneity of PCas might not allow intermediate grades of PCa to be distinguished from aggressive forms using these previously identified miRNA signatures. In this study, we sought to determine the miRNA expression of very high-risk (VHR) PCa and validate this expression pattern in men with differing PCa aggressiveness.

Significance

Serum microRNAs (miRNAs) have emerged as potential noninvasive biomarkers to diagnose prostate cancer (PCa), the most common noncutaneous malignancy among Western men. However, intermediate grades of PCa cannot be distinguished from aggressive forms using current miRNA signatures due to the heterogeneity of PCas. Recently, a high-throughput, spherical nucleic acid-based miRNA expression profiling platform, called the Scano-miR bioassay, was developed to measure the expression levels of miRNAs with both high sensitivity and specificity. By studying serum miRNAs of PCa using the Scano-miR bioassay, we identified a unique molecular signature specific for very high-risk aggressive PCa. This molecular signature will assist in differentiating patients who may benefit from therapy from those who can be closely monitored on active surveillance.

Author contributions: A.H.A., A.W.S., J.J.M., C.S.T., and C.A.M. designed research; A.H.A., A.W.S., J.J.W., and G.F. performed research; A.H.A., A.W.S., and G.F. contributed new reagents/analytic tools; A.H.A., A.W.S., J.J.W., G.F., and C.S.T. analyzed data; and A.H.A., A.W.S., J.J.W., G.F., J.J.M., C.S.T., and C.A.M. wrote the paper.

Reviewers: S.N., Emory University and Georgia Institute of Technology; and N.S., University of Chicago.

The authors declare no conflict of interest.

[1]A.H.A. and A.W.S. contributed equally to this work.

[2]To whom correspondence may be addressed. Email: chadnano@northwestern.edu, joshua.meeks@northwestern.edu, or cthaxton003@northwestern.edu.

This article contains supporting information online at www.pnas.org/lookup/suppl/doi:10.1073/pnas.1611596113/-/DCSupplemental.

Results

Circulating miRNA Profiling Using the Scano-miR Bioassay. Current methods for miRNA profiling include miRNA fluorophore-based microarray techniques, deep sequencing, quantitative real-time PCR (qRT-PCR), and more recently, techniques based upon spherical nucleic acid (SNA) gold nanoparticle conjugates and the Scano-miR platform (26–29). The Scano-miR bioassay, which does not rely on target enzymatic amplification and is therefore amenable to massive multiplexing to screen a sample for thousands of relatively short miRNA targets (19–25 nucleotides), can detect miRNA biomarkers down to 1 femtomolar concentrations with the capability to distinguish perfect miRNA sequences from those with single nucleotide mismatches (i.e., SNPs) (29). We used the Scano-miR platform to study the exosomal miRNA profiles of serum samples from patients with VHR PCa and compared them with the miRNA profiles from healthy individuals and ones with LR PCa. We obtained a discovery set of 16 serum samples from healthy donors and patients with varying grades of PCa (Tables S1 and S2). In a typical Scano-miR assay, exosomes were isolated from serum samples followed by miRNA extraction and ligation to a universal miRNA cloning oligonucleotide linker (29). The ligated mixtures were hybridized onto miRNA microarrays (miR-array), and then SNA probes were added to the miR-arrays to bind the ligated miRNA species. A gold enhancement solution consisting of $HAuCl_4$ and NH_2OH (29, 30) was added to enhance the scattered light signals from the SNA probes. These signals were measured with a Tecan LS Reloaded Scanner and used to extract the miRNA profiles and to determine the miRNA expression levels from each serum sample.

The Scano-miR Molecular Signature Differentiates Clinical Grades of PCa. The comparison between the serum miRNA expression profiles of patients with a high Gleason score (≥ GS 8, HR and VHR, aggressive) compared with control samples with no PCa and patients with a low Gleason score (GS 6, VLR or LR, indolent) identified five exclusively expressed miRNAs. Circulating miR-200c was the most frequently expressed marker (100%) in patients with a high Gleason score ($n = 8$) and was below the detection limit of the Scano-miR assay in all other samples (GS 6 and healthy donors, $n = 8$), whereas miR-219-2-3p, -337-5p, -331-3p, and -409-3p were expressed at different frequencies (75%, 50%, 50%, and 50%, respectively). Importantly, Scano-miR expression analysis identified 58 miRNAs, consisting of 45 experimentally validated miRNAs and 13 predicted miRNAs (Tables S3 and S4), which were coexpressed in all 16 samples. Permutation t tests were performed to identify six differentially expressed miRNAs with significant changes in their expression levels between aggressive and control samples (miR-605, miR-135a*, miR-495, miR-433, miR-371–3p, and miR-106a, with an adjusted P value of 0.0301, 0.0319, 0.0411, 0.0115, 0.0089, and 0.0017, respectively) (Figs. S1 and S2).

Despite the identification of differentially expressed miRNAs, single biomarkers may not be accurate diagnostics for aggressive PCa. For that reason, we calculated the molecular signature score for the differentially expressed miRNAs to distinguish aggressive PCa from control samples using a published mathematical formula described by Zeng et al. (31) The molecular signature analysis revealed that the diagnostic reliability was increased significantly ($P = 0.0036$) upon combining the differentially expressed miRNAs (Fig. 1*A*). The molecular signature score was able to detect 50% of the aggressive PCa samples, which suggests that there might be intermediate grades of PCa that were not distinguished using the Gleason sum of the prostatic needle biopsy specimens. To address this, we performed correlation studies to the clinical pathology of PCa, and we also conducted blinded validation studies using patient serum samples.

Prostate needle biopsies often undergrade the actual tumor aggressiveness, with up to 20% of patients having more aggressive

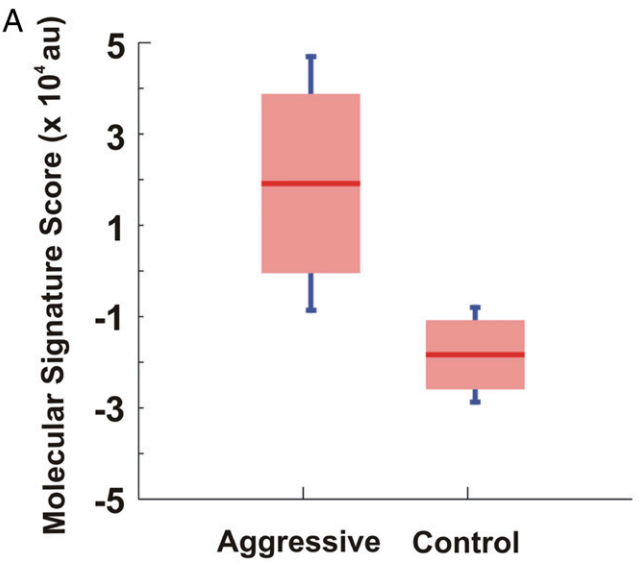

B

Biomarker	Correlation to risk status¶
Molecular Signature	*
hsa-mir-605	*
hsa-mir-135a*	-
hsa-mir-495	*
hsa-mir-433	-
hsa-mir-371-3p	*
hsa-mir-106a	Trend

Fig. 1. Molecular signature score of six miRNAs. (*A*) The molecular signature score was calculated for the six differentially expressed miRNAs using the procedure described in Zeng et al. (31). Distinct ranges of the combined intensity score show that there is little overlap between aggressive and control group expression when using an aggregate score ($P = 0.0036$). (*B*) Aggregate of six miRNAs showing a significant correlation to VHR PCa. The combined signature intensity is correlated to the degree of PCa aggressiveness ($n = 16$). Correlation between miRNA expression and patient risk was analyzed using the Wilcoxon rank-sum test. ¶Correlation P value; $P < 0.1$, Trend; $P < 0.05$, *; no correlation, –.

tumors on subsequent biopsy or prostatectomy (32). Therefore, we investigated the correlation of our identified molecular signature to the clinicopathologic features of PCa following the 2015 National Comprehensive Cancer Network (NCCN) Guidelines for Prostate Cancer (Version 1.2015). To examine such a correlation, prostatic needle biopsy specimens of patients with GS ≥ 8 were grouped into either VHR or HR PCas. Six patients out of eight were identified as having VHR cancer that progressed into locally advanced or metastatic PCa (GS 9, metastasis, and/or clinical stage T3), and the other two patients had HR PCa (GS 8 and clinical stage < T3) (Table S2). Unsupervised hierarchical clustering revealed that these six miRNA markers were able to identify a subclass of four patients out of six, classified as VHR (Fig. S3). We calculated the statistical correlation of the molecular signature and individual miRNAs to the VHR cancer using the

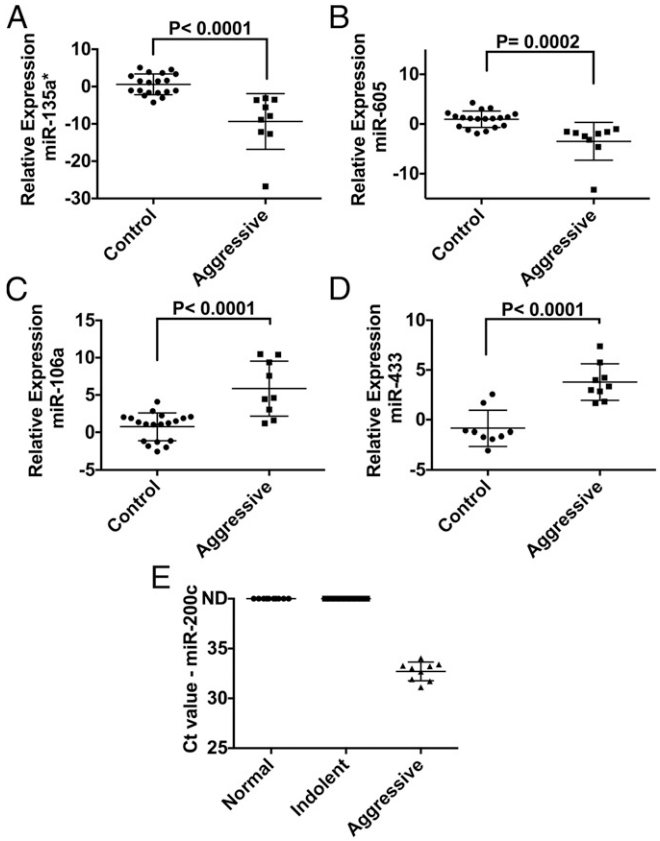

Fig. 2. qRT-PCR validation of the blinded samples. (*A–D*) Blinded qRT-PCR analysis of patient serum samples successfully validated four coexpressed miRNAs (miR-605, miR-135a*, miR-433, and miR-106a) (fold change >1.5). (*E*) Blinded qRT-PCR analysis of a validated, exclusively expressed miRNA: miR-200c.

Kaplan–Meier and Wilcoxon rank-sum tests (33, 34). The results show a significant correlation of the identified molecular signature to the clinical pathology of these patients ($P = 0.041$) (Fig. 1*B*). In contrast, not all differentially expressed miRNAs show high correlations when examined individually (three miRNAs with $P \leq 0.05$), which supports the notion that these individual biomarkers, considered alone, are not uniquely indicative of disease states.

Validation of the Scano-miR miRNA Molecular Signature. To validate the reliability of the identified circulating miRNAs as diagnostic biomarkers, we obtained additional clinical serum samples from deidentified patients (VHR PCa, LR PCa, and healthy donors, with sample size $n = 9$, $n = 9$, and $n = 10$, respectively) and performed a blinded evaluation using qRT-PCR. Within this cohort of nine VHR PCas, we included four patients that were diagnosed with LR tumors but were actually undergraded and had more aggressive tumors at RP. The clinical annotation data for the validation set of samples are included in Table S5. We successfully detected five miRNAs using qRT-PCR (miR-200c, miR-605, miR-135a*, miR-433, and miR-106a) that exhibited the same expression profiles as in our Scano-miR profiling studies using the discovery sample set (Fig. 2 and Fig. S4). Four of these miRNAs (miR-605, miR-135a*, miR-433, and miR-106a) were differentially expressed between VHR and undergraded LR PCas relative to LR PCa samples with fold changes >1.5 (Fig. 2 *A–D*). Circulating miR-433 was differentially expressed in VHR versus LR PCa serum samples (Fig. 2*D*) but was not detected in normal serum samples (Fig. S4). In addition, miR-200c was only detected in serum samples from patients with VHR PCa (Fig. 2*E* and Fig. S4). The data suggest that this miRNA biomarker panel can be used as noninvasive biomarkers to distinguish between patients with VHR and LR forms of PCa.

One of the potential applications of the miRNA score is to accurately risk-stratify patients with biopsy-detected PCa. Thus, we sought to compare the area under the curve (AUC) of our miRNA score compared with the gold standard—the biopsy identified Gleason score—for predicting aggressive compared with indolent cancer. Our receiver operating characteristic (ROC) analyses showed that the miRNAs identified by the Scano-miR bioassay exhibit very high diagnostic capabilities in differentiating between VHR aggressive PCa versus controls with an ROC of 1.0, 0.98, 0.98, 0,92, and 0.89 for miR-200c, miR-433, miR-135a*, miR-605, and miR-106a, respectively (Fig. 3 *A–E*). The prostatic needle biopsy Gleason grading showed the lowest diagnostic capability with an ROC of 0.81 (Fig. 3*F*).

Mapping the validated miRNAs to PCa pathways is important toward understanding their significance in PCa progression. In silico analyses generated a total of 42 candidate pathways (Table S6) from which five common pathways are targeted by the validated miRNA biomarker panel. The identified pathways are primarily involved in cancer progression (including PCa) and phosphatidylinositol-4,5-bisphosphate 3-kinase–Akt serine/threonine kinase (PI3K-Akt) signaling (Table 1). We found the PI3K-Akt signaling pathway to be among the top common candidate pathways, which is a major driver of PCa growth in advanced cancer stages. Additionally, genes that are known to be involved in PCa progression were significant targets of the validated miRNAs (corrected P value threshold of <0.05; Fig. 4). The results suggest that the validated miRNAs target different genes within the same candidate pathways involved in the transition from localized PCa to metastatic PCa.

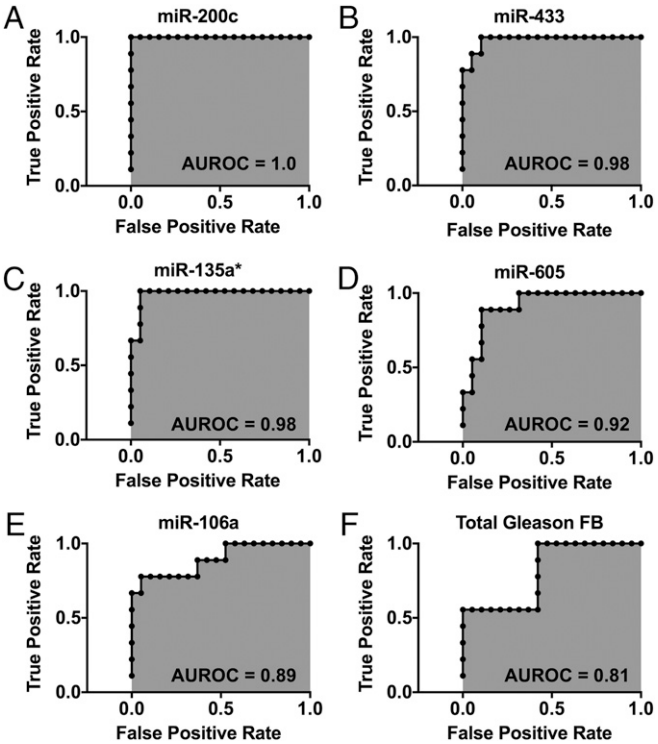

Fig. 3. Specificity and sensitivity analysis. ROC curves were generated to compare the ROC of the Scano-miR miRNAs (*A–E*) to the Gleason sum from the first prostatic needle biopsy (FB) (*F*). The miRNAs identified by the Scano-miR bioassay yielded an ROC of at least 0.89 in differentiating between VHR PCa versus control group.

Table 1. Common KEGG pathways

KEGG pathway	*P* value	No. of genes	No. of miRNA
Pathways in cancer, hsa05200	2.94E-06	44	5
PI3K-Akt signaling pathway, hsa04151	5.51E-06	44	5
PCa, hsa05215	1.06E-05	17	5
Focal adhesion, hsa04510	1.93E-03	26	5
Glioma, hsa05214	1.36E-02	11	5

The table shows the biological pathways shared with the five validated miRNA PCa biomarkers.

Discussion

Risk stratified treatment of PCa is critically dependent on staging through PSA, physical examination, and tissue biopsy. To address the inherent gaps in cancer staging, we successfully applied and validated the Scano-miR profiling platform and ultimately identified a unique panel of miRNA biomarkers associated with different grades of PCa.

The miRNA biomarker panel was discovered and validated by investigation of the serum miRNA profiles from two experimental sample sets. The first set was profiled using the Scano-miR bioassay to identify differentially expressed miRNAs specific to VHR PCa samples that were previously clinically graded based upon Gleason biopsy scoring. A blinded qRT-PCR study was then performed on the second sample set, which served to validate the identified miRNA biomarkers in patient samples with known pathological grading. For example, although individual miRNA biomarkers such as miR-433 and miR-135a* did not fully agree with the clinical grading of PCa, known pathological grading of the blinded qRT-PCR study validated the significant diagnostic capabilities of the identified miRNA biomarkers including circulating miR-433 and miR-135a*. The molecular signature generated from the validated miRNAs enabled us to accurately distinguish between patients with indolent or aggressive forms of PCa at rates higher than typical prostatic needle biopsy Gleason scoring. This miRNA biomarker panel represents a simple tool for the diagnosis of PCa without the need for surgical intervention.

The majority of the identified miRNAs were linked previously to the pathogenesis of PCa either as oncogenes or tumor suppressors. Circulating miR-200c in plasma can be used as a marker to distinguish localized PCa from metastatic castration-resistant PCa (25). miR-106a was significantly dysregulated in PCa, whereas a single nucleotide polymorphism in miR-605 was found to correlate with the biochemical recurrence of PCa (35, 36). However, to our knowledge, circulating miR-433 and miR-135a* have not been linked to PCa previously, and the selected miRNA panel (miR-200c, miR-605, miR-135a*, miR-433, and miR-106a) has not been proposed to have a predictive value for the management of PCa.

Identifying genetic clues to the molecular basis of PCa growth is a major challenge, as the number of mutated genes is often higher than the actual mutations that drive cancer. Our analysis with the selected miRNA panel in the PCa pathway suggested a list of target genes [Phosphatase and Tensin Homolog (*PTEN*), *PI3K*, Tumor Protein p53 (*TP53*), Retinoblastoma 1 (*RB1*), *MDM2*, *TGFA*, *NFKB1*, *CASP9*, *CDKN1A*, *E2F1*, *SOS1*, *MAPK1*, *CREB5*, *TCF7L1*, *CCND1*, *BCL2*, *PDGFD*, *PDGFRA*, *GRB2*, *LEF1*, and *TCF4*]. Although many of these target genes might act as passengers, some of them are known drivers of PCa tumorigenesis. For example, somatic mutations of TP53 and RB1 in PCa are well-established genetic alterations (37). Loss of the tumor suppressor PTEN causes activation of the PI3K-Akt signaling pathway, which is a critical oncogenic pathway in PCa (38). The PI3K-Akt pathway is an important driver of epithelial–mesenchymal transition (EMT) to reduce intercellular adhesion of cancer cells while increasing motility (39). Recent reports suggest a cross-talk between PI3K-AKT and the androgen receptor (AR) pathway in PCa with an inactivated PTEN gene (40), where activated PI3K/AKT causes PCa to become metastatic and hormone-independent. As a result, the validated miRNAs might play an important role in the regulation of aggressive PCa.

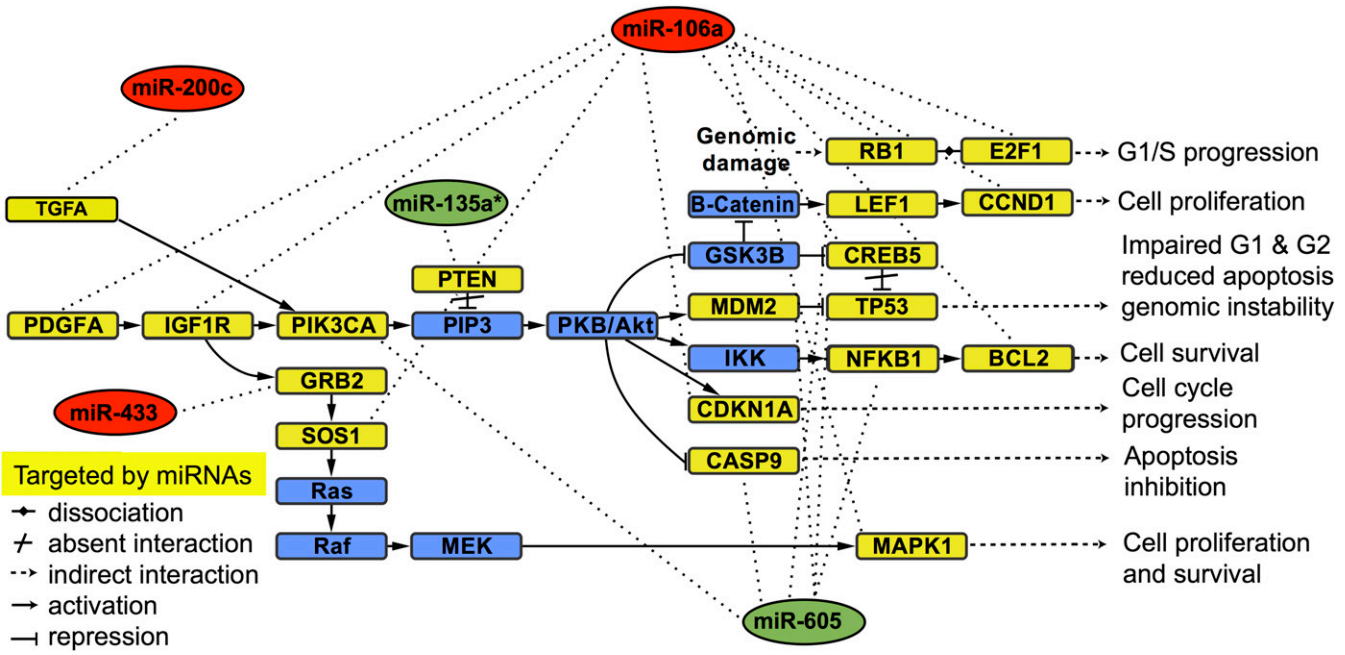

Fig. 4. KEGG pathway analysis of the validated miRNAs. Target genes and biological pathways for up-regulated miRNAs (red oval) and down-regulated miRNAs (green oval) were identified using microT-CDS and TarBase to classify the GO category and KEGG pathway enrichment with a corrected *P* value threshold of <0.05. The yellow squares represent target genes potentially altered by the expression of the validated miRNAs, and blue squares represent genes that are not directly targeted by the validated miRNAs.

In conclusion, we have identified circulating miRNAs that serve as a molecular signature to detect VHR PCa. These biomarkers (miR-200c, miR-605, miR-135a*, miR-433, and miR-106a) showed significant correlation to VHR PCa in clinical samples. This work serves as an initial proof-of-principle study that circulating miRNA biomarkers can identify specific grades of PCa, and further investigations with larger numbers of patient samples are currently underway to validate the utility of using these biomarkers and scoring signature to unambiguously diagnose the disease. Finally, additional work will be required to determine the role of the identified serum miRNAs in PCa development and tumorigenesis.

Materials and Methods

Clinical Samples. The discovery set of serum samples were purchased from two vendors, as specified in Table S1 (ProteoGenex, Inc. and ProMedDx, LLC). The validation set of serum samples with different grades of PCas and negative for metastasis were obtained from the Northwestern University (NU) Prostate Specialized Programs of Research Excellence (SPORE) serum repository following the institutional review protocol, whereas healthy serum samples were purchased from BioreclamationIVT. Serum samples were collected from donors with matched ethnicity and sex (Caucasian and male). Samples were stored at –80 °C upon arrival and thawed on ice before use.

Isolation of Serum Exosomal RNA. Exosomes were isolated from the discovery set of serum samples using ExoQuick Exosome Precipitation Solution (System Biosciences, part #EXOQ5A-1) following the manufacturer's protocol. In short, serum samples were centrifuged to remove cell debris (3,000 rpm, 15 min) (Eppendorf Centrifuge 5424R, rotor FA-45-24-11). We added 1 mL serum supernatant to 252 μL ExoQuick exosome precipitation solution and mixed and incubated it at 4 °C for 30 min. Following incubation, the mixture was recentrifuged and the exosome pellet was collected. RNA isolation from the exosome pellet was performed using mirVana PARIS miRNA isolation kit (Ambion, part #AM1556) following the manufacturer's protocol by suspending the exosome pellet in 300 μL of cell disruption buffer solution followed by adding 300 μL of 2× denaturing solution and was allowed to incubate on ice for 5 min. Next, 600 μL of acid-phenol:chloroform was added to the mixture, vortexed, and centrifuged to collect 300 μL of the aqueous phase (10,000 rpm, 5 min). The aqueous phase was mixed with 100% ethanol at a 1:1.25 volume ratio and then column filtered, followed by RNA elution with 100 μL of elution buffer. Total RNA from the filtrate was precipitated by adding 0.3 M NaCl, 20 μg glycogen, and 1 volume of isopropanol and allowed to incubate at –80 °C for 12 h. The mixture was centrifuged to collect the pellet (15,000 rpm, 30 min, 4 °C), followed by one wash with 1 mL of 70% (vol/vol) ethanol. The pellet was washed once with 1 mL 70% ethanol, air-dried, and suspended in 10 μL RNase-free water. Total RNA was stored at –80 °C until profiling studies using the Scano-miR bioassay.

Synthesis of the Universal SNA Nanoconjugates. SNAs were synthesized by chemisorbing 4 μM of a propylthiol-modified ssDNA recognition sequence [5′-propylthiol-$(A)_{10}$-TCCTTGGTGCCCGAGTG-3′] complementary to miRNA Cloning Linker II (IDT) onto 10 nM of citrate-stabilized gold nanoparticles (13 nm in diameter) following a published protocol (29). The mixture was allowed to incubate for 1 h at room temperature, followed by a salt aging process consisting of 0.01% SDS, 10 mM phosphate buffer (pH 7.4), and 0.1 M sodium chloride (NaCl), for an additional 1 h at room temperature. Two additional aliquots of 0.1 M NaCl were added, and the mixture was allowed to incubate for 1 h between each addition and subsequently incubated overnight (room temperature, shaking at 130 rpm). SNAs were purified through three successive rounds of centrifugation (16,000 × *g* for 20 min), supernatant removal, and resuspension in PBS (137 mM NaCl, 10 mM phosphate, 2.7 mM KCl, pH 7.4). All experiments were carried out with RNase-free materials.

miRNA Profiling Using the Scano-miR Platform. Isolated serum miRNAs were added to a ligation mixture (200 U Truncated T4 RNA Ligase 2, 900 ng miRNA cloning linker II, 12% PEG 8000, and 1× T4 RNL2 buffer) from New England Biolabs following the manufacturer's protocol and allowed to incubate for 3 h at 37 °C. The ligation mixture was suspended in 400 μL RNase-free 2× SSC hybridization buffer (0.3 M NaCl, 0.03 M sodium citrate, pH 7.0) and hybridized onto NCode Human miRNA microarray V3 (Invitrogen) for 12 h at 52 °C (29). Following the incubation, the miR-arrays were washed to remove unbound miRNAs using prewarmed 2× SSC (52 °C), 2× SSC, PBS (137 mM NaCl, 10 mM phosphate, 2.7 mM KCl, pH 7.4), and nanopure water. We hybridized 1 nM of the synthesized SNAs suspended in 400 μL 2× SSC onto the miR-array at 56 °C for 1 h. The washing steps were repeated to remove unreacted SNAs. All experiments were performed using RNase-free materials. Finally, the light scattering of the gold nanoparticles was increased using three rounds of gold enhancing solution [a freshly mixed 1:1 (vol/vol) solution of 1 mM $HAuCl_4$ and 10 mM NH_2OH] (5 min each, at room temperature). The miR-array was imaged with a LS Reloaded scanner (Tecan).

Data Analysis and miRNA Clustering. Raw Scano-miR expression data were extracted from 4,608 probes using GenePix Pro-6 software (Molecular Devices). Expression values below background threshold as well as abnormal probe shape index were filtered from downstream data analysis. An average of three probe replicates per miRNA target were used for expression analysis. In total, 705 human miRNAs were screened for each sample. The identities and frequencies of the expression profiles were calculated for five exclusively expressed miRNAs that were detected solely in aggressive serum samples, where frequency denotes the number of times the miRNA was detected in the serum sample divided by the number of aggressive samples. We filtered 583 miRNAs that were not expressed in all 16 samples from further expression analysis. Quantile normalization was performed on 16 samples with 167 coexpressed features. Heat maps were clustered using Pearson correlation as a distance metric and visualized using MATLAB.

Molecular Signature and Clinical Analysis. A permutation *t* test was performed to obtain six differentially expressed miRNAs between aggressive and control samples. Permutation *t* tests were used to estimate the null distribution of the *t* test statistic (41). *P* values were corrected for false discovery rate (FDR) using the Storey–Tibshirani procedure (41). A molecular signature score was calculated based on the differences between the expression levels of down-regulated and up-regulated miRNAs using a published formula (31). The Kaplan–Meier and Wilcoxon rank-sum tests were used to assess the correlation of the signature score and individual miRNA to HR patient profiles.

qRT-PCR Validation of the Blinded Samples. The serum exosomes were isolated from the validation set of serum samples using the previously described protocol and suspended in a denaturing lysis buffer (Ambion, part #AM1560). We spiked 100 pM of synthetic cel-miR-40-3p (Applied Biosystems, part #MC10631) into denatured exosomes. RNA isolation from the denatured exosome was performed using mirVana miRNA isolation kit (Ambion, part #AM1560) following the manufacturer's protocol. Using TaqMan RT kit (part #4366597), TaqMan hsa-miR-200c, hsa-miR-106a, hsa-miR-605, hsa-miR-371-3p, hsa-miR-135a*, hsa-miR-433, hsa-miR-495, and cel-miR-40 RT primers, 1 ng (5 μL) of total RNA from each sample was reverse-transcribed in 15 μL reaction volumes following the manufacturer's protocol (Applied Biosystems, TaqMan MicroRNA Assays PN 4364031E). qRT-PCR reactions were conducted in 96-well plates with 1.33 μL of RT product with TaqMan PCR master mix (part #4364343) and TaqMan probes for each miRNA in a total volume of 20 μL. An ABI Prism Model 7900 HT instrument was used to perform the qRT-PCR reactions with data analyzed using the comparative Ct method with cel-miR-40-3p used as an exogenous control. Known concentrations of cel-miR-40-3p were used to generate qRT-PCR standard curve. For statistical evaluation of the qRT-PCR validation test, the Mann–Whitney *t* test was used, where a *P* value less than 0.05 and a cutoff of >1.5-fold change was considered statistically significant (GraphPad Prism 6).

Sensitivity and Specificity Calculation. The tradeoff between sensitivity (true positive rate) and false positive rate (1-specificity) using the Gleason scoring sum of the first prostatic needle biopsy (FB), individual miRNA biomarkers, and molecular signature score for predicting VHR PCa was assessed using the area under the ROC curve.

Target Genes and Pathway Analysis of the Validated miRNAs. In silico analysis was performed to identify miRNA target genes and molecular pathways potentially altered by the expression of single or multiple miRNAs. Putative target genes of miRNA were determined using the homology search algorithm microT-CDS and a database of published, experimentally validated miRNA-gene interactions, TarBase (42, 43). For microT-CDS, a microT prediction threshold of >0.8 was set. DIANA-miRPath was used to perform functional annotation clustering and pathway enrichment analysis of multiple miRNA target genes (44). Two-sided Fisher's exact test and the X^2 test were used to classify the Gene Ontology (GO) category and KEGG pathway enrichment, and the FDR was calculated to correct *P* values. A corrected *P* value threshold of <0.05 was used to select significant GO categories and KEGG pathways.

ACKNOWLEDGMENTS. The research was supported by the Prostate Cancer Foundation and the Center for Cancer Nanotechnology Excellence (CCNE) initiative of the National Institutes of Health (NIH) under Awards U54 CA151880 and U54 CA199091. A.H.A. acknowledges the King Abdullah Scholarships Program funded by the Ministry of Higher Education of Saudi Arabia for doctoral scholarship support. C.S.T. and J.J.M. acknowledge the Northwestern Memorial Foundation Dixon Translational Research Grant Initiative Award SP0010333. J.J.M is supported by National Cancer Institute (NCI) SPORE Grant P50 CA180995. The contributions of G.F. are partially supported by NCI Cancer Center Support Grant NCI CA060553 and National Center for Advancing Translational Sciences Grant 8UL1TR000150. J.J.W. was supported in part by National Science Foundation (NSF) Grants DGE-1007911 and NIH T32 GM008449. Any opinions, findings, and conclusions or recommendations expressed in this material are those of the author(s) and do not necessarily reflect those of the sponsors.

1. Jemal A, et al. (2007) Cancer statistics, 2007. *CA Cancer J Clin* 57(1):43–66.
2. Siegel RL, Miller KD, Jemal A (2015) Cancer statistics, 2015. *CA Cancer J Clin* 65(1):5–29.
3. Heijnsdijk EA, et al. (2009) Overdetection, overtreatment and costs in prostate-specific antigen screening for prostate cancer. *Br J Cancer* 101(11):1833–1838.
4. Grubb RL, 3rd, et al.; PLCO Project Team (2009) Serum prostate-specific antigen hemodilution among obese men undergoing screening in the Prostate, Lung, Colorectal, and Ovarian Cancer Screening Trial. *Cancer Epidemiol Biomarkers Prev* 18(3):748–751.
5. Andriole GL, et al.; PLCO Project Team (2009) Mortality results from a randomized prostate-cancer screening trial. *N Engl J Med* 360(13):1310–1319.
6. Crawford ED, Andriole GL, Marberger M, Rittmaster RS (2010) Reduction in the risk of prostate cancer: Future directions after the Prostate Cancer Prevention Trial. *Urology* 75(3):502–509.
7. Schröder FH, et al.; ERSPC Investigators (2009) Screening and prostate-cancer mortality in a randomized European study. *N Engl J Med* 360(13):1320–1328.
8. Epstein JI (2010) An update of the Gleason grading system. *J Urol* 183(2):433–440.
9. Hugosson J, et al. (2010) Mortality results from the Göteborg randomised population-based prostate-cancer screening trial. *Lancet Oncol* 11(8):725–732.
10. Schröder FH, et al.; ERSPC Investigators (2012) Prostate-cancer mortality at 11 years of follow-up. *N Engl J Med* 366(11):981–990.
11. Conti SL, et al. (2009) Pathological outcomes of candidates for active surveillance of prostate cancer. *J Urol* 181(4):1628–1633, discussion 1633–1634.
12. Klotz L, et al. (2015) Long-term follow-up of a large active surveillance cohort of patients with prostate cancer. *J Clin Oncol* 33(3):272–277.
13. Bostwick DG, Myers RP, Oesterling JE (1994) Staging of prostate cancer. *Semin Surg Oncol* 10(1):60–72.
14. Isariyawongse BK, et al. (2008) Significant discrepancies between diagnostic and pathologic Gleason sums in prostate cancer: The predictive role of age and prostate-specific antigen. *Urology* 72(4):882–886.
15. Chun FK, et al. (2010) Optimizing performance and interpretation of prostate biopsy: A critical analysis of the literature. *Eur Urol* 58(6):851–864.
16. Barbieri CE, et al. (2013) The mutational landscape of prostate cancer. *Eur Urol* 64(4): 567–576.
17. Lee RC, Feinbaum RL, Ambros V (1993) The *C. elegans* heterochronic gene *lin-4* encodes small RNAs with antisense complementarity to *lin-14*. *Cell* 75(5):843–854.
18. Lim LP, et al. (2005) Microarray analysis shows that some microRNAs downregulate large numbers of target mRNAs. *Nature* 433(7027):769–773.
19. Lewis BP, Burge CB, Bartel DP (2005) Conserved seed pairing, often flanked by adenosines, indicates that thousands of human genes are microRNA targets. *Cell* 120(1):15–20.
20. Mitchell PS, et al. (2008) Circulating microRNAs as stable blood-based markers for cancer detection. *Proc Natl Acad Sci USA* 105(30):10513–10518.
21. Selth LA, et al. (2012) Discovery of circulating microRNAs associated with human prostate cancer using a mouse model of disease. *Int J Cancer* 131(3):652–661.
22. Valadi H, et al. (2007) Exosome-mediated transfer of mRNAs and microRNAs is a novel mechanism of genetic exchange between cells. *Nat Cell Biol* 9(6):654–659.
23. Alhasan AH, Patel PC, Choi CHJ, Mirkin CA (2014) Exosome encased spherical nucleic acid gold nanoparticle conjugates as potent microRNA regulation agents. *Small* 10(1): 186–192.
24. Brase JC, et al. (2011) Circulating miRNAs are correlated with tumor progression in prostate cancer. *Int J Cancer* 128(3):608–616.
25. Watahiki A, et al. (2013) Plasma miRNAs as biomarkers to identify patients with castration-resistant metastatic prostate cancer. *Int J Mol Sci* 14(4):7757–7770.
26. Grasedieck S, et al. (2013) Circulating microRNAs in hematological diseases: Principles, challenges, and perspectives. *Blood* 121(25):4977–4984.
27. Mirkin CA, Letsinger RL, Mucic RC, Storhoff JJ (1996) A DNA-based method for rationally assembling nanoparticles into macroscopic materials. *Nature* 382(6592): 607–609.
28. Taton TA, Mirkin CA, Letsinger RL (2000) Scanometric DNA array detection with nanoparticle probes. *Science* 289(5485):1757–1760.
29. Alhasan AH, et al. (2012) Scanometric microRNA array profiling of prostate cancer markers using spherical nucleic acid-gold nanoparticle conjugates. *Anal Chem* 84(9): 4153–4160.
30. Kim D, Daniel WL, Mirkin CA (2009) Microarray-based multiplexed scanometric immunoassay for protein cancer markers using gold nanoparticle probes. *Anal Chem* 81(21):9183–9187.
31. Zeng X, et al. (2012) Circulating miR-17, miR-20a, miR-29c, and miR-223 combined as non-invasive biomarkers in nasopharyngeal carcinoma. *PLoS One* 7(10):e46367.
32. Dijkstra S, Hamid AR, Leyten GH, Schalken JA (2012) Personalized management in low-risk prostate cancer: The role of biomarkers. *Prostate Cancer* 2012(327104): 327104.
33. Kaplan EL, Meier P (1958) Nonparametric estimation from incomplete observations. *J Amer Statist Assn* 53(282):457–481.
34. Mann HB, Whitney DR (1947) On a test of whether one of two random variables is stochastically larger than the other. *Ann Math Stat* 18(1):50–60.
35. Volinia S, et al. (2006) A microRNA expression signature of human solid tumors defines cancer gene targets. *Proc Natl Acad Sci USA* 103(7):2257–2261.
36. Huang SP, et al. (2014) Genetic variants in microRNAs and microRNA target sites predict biochemical recurrence after radical prostatectomy in localized prostate cancer. *Int J Cancer* 135(11):2661–2667.
37. Sellers WR, Sawyers CA (2002) Somatic genetics of prostate cancer: Oncogenes and tumor suppressors. *Prostate Cancer: Principles and Practice*, ed Kantoff PW (Lippincott Williams & Wilkins, Philadelphia, PA), 1st Ed, pp 53–76.
38. Majumder PK, Sellers WR (2005) Akt-regulated pathways in prostate cancer. *Oncogene* 24(50):7465–7474.
39. Larue L, Bellacosa A (2005) Epithelial-mesenchymal transition in development and cancer: Role of phosphatidylinositol 3′ kinase/AKT pathways. *Oncogene* 24(50): 7443–7454.
40. Marques RB, et al. (2015) High efficacy of combination therapy using PI3K/AKT inhibitors with androgen deprivation in prostate cancer preclinical models. *Eur Urol* 67(6):1177–1185.
41. Storey JD, Tibshirani R (2003) Statistical significance for genomewide studies. *Proc Natl Acad Sci USA* 100(16):9440–9445.
42. Reczko M, Maragkakis M, Alexiou P, Grosse I, Hatzigeorgiou AG (2012) Functional microRNA targets in protein coding sequences. *Bioinformatics* 28(6):771–776.
43. Vlachos IS, et al. (2015) DIANA-TarBase v7.0: Indexing more than half a million experimentally supported miRNA:mRNA interactions. *Nucleic Acids Res* 43(Database Issue):D153–D159.
44. Vlachos IS, et al. (2012) DIANA Mirpath V.2.0: Investigating the combinatorial effect of microRNAs in pathways. *Nucleic Acids Res* 40(Web Server Issue):W498–W504.